A Solution Synthetic Route to Nanophase Cobalt Film and Sponge

Å. Ekstrand,[†] K. Jansson,[‡] and G. Westin*,[†]

Department of Materials Chemistry, Ångström Laboratory, Uppsala University, SE-751 21 Uppsala, Sweden, and Department of Inorganic Chemistry, Arrhenius Laboratory, Stockholm University, SE-106 91 Stockholm, Sweden

Received March 31, 2004. Revised Manuscript Received October 13, 2004

An efficient, low-cost solution-chemical route to nanophase cobalt as dense films and sponges has been developed. $Co(NO_3)_2 \cdot 6H_2O$ and $Co(OAc)_2 \cdot 4H_2O$ were mixed with triethanolamine in methanol, and the solution was evaporated in air to a viscous liquid. Heating at 10 °C min^{-1} to 470 and 500 °C yielded highly porous sponges consisting of 3−6 and 9−11 nm sized face centered cubic (fcc) cobalt crystallites, respectively. Spin-coating on alumina and aluminum substrates with a 1 M Co-precursor solution and subsequent heating at 10 °C min^{-1} to 500 °C yielded dense films of <20 nm sized fcc cobalt crystallites. The microstructural and compositional evolution process on heating to form the cobalt metal was studied by TGA, DTA, and FT-IR spectroscopy, powder X-ray diffraction, TEM-EDS, and SEM-EDS. The C, N, and O contents could be kept low, 0.5, 0.02, and 0.2 wt %, respectively, at 700 °C, but the carbon content could also reproducibly be adjusted to up to 13 wt % C in excess, by varying the precursor composition.

Introduction

Cobalt is a very versatile metallic material, with broad areas of application due to its chemical, catalytic, and magnetic properties. Despite its wide range of use, however, there are few efficient techniques to produce functional structures such as nanophase films or porous materials of very high surface area. Thin films of cobalt attract much current interest due to their magnetic properties, which depend on the particle size, going from ferromagnetic for large Co particles in bulk to superparamagnetic for isolated and extremely small particles. Giant magnetoresistance (GMR) has been found in multilayered films containing Co and, for example, Cu.[1−3] Most approaches to the production of thin nanostructured films are based on physical processes, for example, thermal evaporation, magnetron and Ar^+-ion sputtering, and pulsed laser deposition,[4−8] but chemical vapor deposition,[9,10] electrochemical deposition,[11−14] and nebulized spray pyrolysis deposition have also been used.[15] Most of these techniques require special conditions and equipment and are therefore relatively expensive and inappropriate for large-scale production. The physical processes often encounter difficulties with deposition on large or nonflat surfaces, whereas electrochemical deposition often has problems with irregular deposition and nonconducting substrates, which reduces its versatility. While nebulized spray pyrolysis appears to have potential for large-scale application on extended substrates, it does not seem to yield dense films or ultrasmall nanocrystallites.[15] The substrate characteristics are often a strongly determining factor for the outcome in most of these processes.

Metal sponges consisting of nanoparticles are of great interest when a large surface area is crucial for the rate of chemical or electrochemical reactions, as in catalysts and battery electrodes.[3] In the latter case, good conductivity through the electrode material is of great importance for the performance, and in the former case a nonbrittle support that can be consumed to some extent without loss of the active catalyst at the surface, thus increasing the lifetime, should be advantageous. Cobalt catalysts on various forms of supports are utilized in the economically important Fischer−Tropsch catalytic processing of low-branched hydrocarbons, and development is still in progress, mainly toward lowering

* Corresponding author. E-mail: gunnar.westin@mkem.uu.se.
[†] Uppsala University.
[‡] Stockholm University.

(1) Grundy, P. J.; Pollard, R. J.; Tomlinson, M. E. *J. Magn. Magn. Mater.* **1993**, *126*, 516−518.
(2) Parkin, S. S. P.; Li, Z. G.; Smith, D. J. *J. Appl. Phys. Lett.* **1991**, *58*, 2710−2713.
(3) Ashby, M. F.; Evans, A.; Norman, A. F.; Gibson, L. J.; Hutchinson, J. W.; Wadely, H. N. G. *Metal Foams A Design Guide*; Butterworth-Heinemann: Woburn, MA, 2000.
(4) Dureuil, V.; Ricolleau, C.; Gandais, M.; Grigis, C.; Lacharme, J. P.; Naudon, A. *J. Cryst. Growth* **2001**, *233*, 737−748.
(5) Giovanardi, C.; Luches, P.; di Bona, A.; Borghi, A.; Valeri, S. *Thin Solid Films* **2001**, *397*, 116−124.
(6) Sellmann, R.; Fritzsche, H.; Maletta, H. *Surf. Sci.* **2001**, *1−2*, 185−194.
(7) Thiele, J.; Belkhou, R.; Bolou, O.; Heckman, O.; Magnan, H.; Le Fèvre, P.; Chandesris, D.; Guillot, C. *Surf. Sci.* **1997**, *384*, 120−128.
(8) Phakomov, A. B.; Denardin, J. C.; de Lima, O. F.; Knobel, M.; Missell, F. P. *J. Magn. Magn. Mater.* **2001**, *226−230*, 1631−1632.
(9) Mane, A.; Shalini, K.; Devi, A.; Lakshmi, R.; Dharmaprakash, M. S.; Pranjape, M.; Shivashankar, S. A. *MRS Symp. Proc.* **2000**, *615*, G6111−G6116.
(10) Gu, S.; Atanasova, P.; Hampden-Smith, M. J.; Kodas, T. T. *Thin Solid Films* **1999**, *340*, 45−52.
(11) Pasa, A. A.; Schwarzacher, W. *Phys. Status Solidi* **1999**, *173*, 73.
(12) Kleinert, M.; Weibel, H.-F.; Engelmann, G. E.; Martin, H.; Kolb, D. M. *Electrochim. Acta* **2001**, *46*, 3129−3136.
(13) Munford, M. L.; Seligman, L.; Sartorelli, M. L.; Voltolini, E.; Martins, L. F. O.; Schwarzacher, W.; Pasa, A. A. *J. Magn. Magn. Mater.* **2001**, *226−230*, 1613−1615.
(14) Kudo, K.; Kobayakawa, K.; Sato, Y. *Electrochim. Acta A* **2001**, *47*, 353−357.
(15) Parashar, S.; Raju, A. R.; Rao, C. N. R. *Mater. Chem. Phys.* **1999**, *61*, 46−49.

10.1021/cm0494610 CCC: $30.25
Published on Web 12/14/2004

the reaction temperatures by reduction of particle size.[16,17] Very few routes to high-surface-area nanostructured porous materials have been reported, and those we found in the literature all used some kind of inorganic or organic template. Thus, microporous films with highly ordered pore structures were produced by electrodeposition of cobalt on polymeric spheres and subsequent dissolution and removal of the polymer template,[18] and etched polycarbonate or alumina membranes used as templates for the electrodeposition yielded arrays of wires.[19] Although these techniques offer good control of the pore-size distribution and of the cobalt particle shape and arrangements in films, they are not suitable for large-scale low-cost production and they apparently do not yield ultrasmall cobalt nanocrystallites in the sub 10−20 nm range. Thus, it seems that there is presently no efficient route to porous cobalt consisting of particles small enough to give the extremely high surface areas needed in catalysis and electrodes or for nanophysics to play an important role. Ductile nanocrystalline sponges may also be suitable for compaction into three-dimensional bodies of very fine-grained cobalt with special chemical, mechanical, and magnetic properties, although grain-growth and reduced density may constitute problems depending on the application in mind.

Herein, we describe a novel solution-chemical route, first developed by us for preparation of nickel films and sponges,[20] to cobalt sponges and films consisting of crystallites in sizes below 20 nm. It uses only simple inorganic salts and requires heating to less than 500 °C. The microstructural and compositional evolution process on heating to form the cobalt metal was studied by means of TGA, DTA, FT-IR spectroscopy, powder and film X-ray diffraction, TEM-EDS, and SEM-EDS. The carbon content could reproducibly be adjusted by varying the precursor composition, and the N and O levels could be held very low.

Experimental Section

Chemicals and Equipment Used. Methanol (Merck p.a.), $Co(OAc)_2 \cdot 4H_2O$ (Acros, 99%), $Co(NO_3)_2 \cdot 6H_2O$ (Fluka, >99.0%), and triethanolamine (Fluka, 99%) were all used as purchased.

The microstructures were analyzed and electron diffraction (ED) patterns were obtained with a transmission electron microscope (TEM, JEOL 2000 FXII) equipped with an energy-dispersive spectrometer (EDS, Link 10000AN), and also with scanning electron microscopes (SEM, JEOL 820 and JEOL SEM 880) equipped with energy-dispersive spectrometers (EDS, Link 10000AN and Link Isis, respectively). The powders were characterized by X-ray diffraction (PXRD) with a Guiner-Hägg geometry camera, using Cu $K\alpha_1$ radiation and Si as internal standard, and the films were characterized with 2θ scans using a diffractometer (Siemens D-5000), with Cu $K\alpha$ radiation. The weight-loss of the precursor material on heating was studied with a thermogravimetric apparatus (TGA, Perkin-Elmer TGA7) and a differential thermal analyzer (DTA, Setaram Labsys 1600) in nitrogen or argon atmosphere. The cobalt powders obtained in the TG apparatus were rapidly transferred to a glovebox with a dry oxygen-free atmosphere and kept in sealed vials until investigated. To avoid air-oxidation in connection with the transfer of the sample to the TEM, special precautions were made. The holy carbon Cu-grid was loaded with powdered cobalt sponge inside the glovebox and mounted into the sample holder, which was in its turn put in a box inside a plastic bag. The box in the closed bag was transported to the TEM and opened inside another plastic bag connected to the TEM under flowing nitrogen, and inserted into the TEM. The average C, N, and O contents of the bulk samples were determined at an external analytical laboratory specialized in the analysis of metals and carbides, using standard combustion-spectroscopic methods. The analyses performed with LECO instruments had an accuracy of approximately 0.03 wt % for O, C, and N. In practice, the error is larger in the present materials due to experimental difficulties such as oxidation sensitivity. The measured contents for a double sample of the 1:0 composition were within 0.02 wt % from the average, while for high $OAc:NO_3$ ratios of 4:1, 2:1, 1:1, and 1:2 with 2−4 different samples on each composition, the results varied within 0.2−1.2 wt % units from average. SEM-EDS (JEOL 880 with "window-less" EDS) was used to some extent for O, C, and N analysis, but this technique is much less sensitive and accurate than the elemental analysis, and the porous sponge geometry is far from an ideal geometry for EDS analysis, which is why this method was used for qualitative analysis only. In addition, the oxides on the metal surfaces could be detected in small amounts with IR spectroscopy and TEM-ED. The compositions of the precursor concentrates and the powders obtained by heat-treatment at various temperatures were investigated with a Fourier transform infrared spectrometer (FT-IR, Bruker IFS-55), in the range 5000−370 cm^{-1}. The precursor concentrates were studied as paraffin mulls between KBr plates, and all other samples were studied as liquids between KBr plates or as KBr tablets. The peaks due to the paraffin were successfully subtracted in the range 2700−370 cm^{-1}, whereas the peaks at 3000−2700 cm^{-1} could not be properly removed.

Synthesis of Cobalt Metal. *WARNING*: Although, despite many syntheses made with different batch sizes, from milligrams to several tens of grams without explosions or self-ignition during drying, any mixture of nitrates and acetates should be regarded as potentially explosive, especially in large batches. The metal sponges when prepared in gram-scale may glow from oxidation when taken out in air at temperatures above ca. 100 °C, resulting in a complete conversion to CoO, but the oxidation is slow at room temperature.

$Co(NO_3)_2 \cdot 6H_2O$ and $Co(OAc)_2 \cdot 4H_2O$ were mixed in different molar ratios, from pure nitrate to pure acetate; the mixtures were dissolved in methanol to a total cobalt concentration of 0.5 M, and 0.5 TEA/Co was added. The solutions were then evaporated in air to sticky liquid concentrates for sponge preparation, and to a cobalt concentration of ca. 1 M for film preparation, at temperatures in the range 20−35 °C. The evaporations were normally made with a slow stream of pressurized air, but slow evaporation from Petri dishes standing in a hood could also be made.

The thermal decomposition of the nitrate and organic groups to form a cobalt sponge was monitored by heat-treatment in the TG apparatus under nitrogen gas, using different heating-rates to temperatures up to 900 °C. The samples obtained from these heat-treatments were studied by PXRD, FT-IR spectroscopy, SEM, and TEM. Larger, multigram size batches were prepared under flowing nitrogen in a pit-furnace by heating at 10 °C min^{-1} to 700 °C and were investigated by elemental analysis, using standard chemical and spectrometric techniques, PXRD and SEM. The SEM and

(16) Iglesia, E. *Appl. Catal., A* **1997**, *161*, 59−78.
(17) Sun, S.; Tsubaki, N.; Fujimoto, K. *Appl. Catal., A.* **2000**, *202*, 121−131.
(18) Bartlett, P. N.; Birkin, P. R.; Ghanem, M. A. *Chem. Commun.* **2000**, *6*, 1671−1672.
(19) Schwanbech, H.; Schmidt, U. *Electrochim. Acta* **2000**, *45*, 4389−4398.
(20) Ekstrand, Å.; Jansson, K.; Westin, G. *J. Sol.-Gel Sci. Technol.* **2000**, *19*, 353−356.

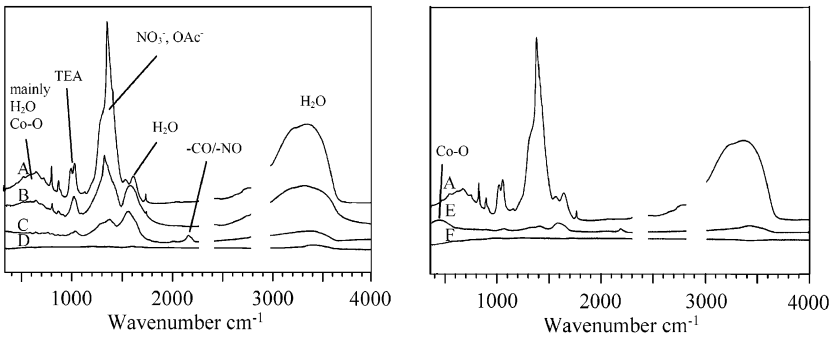

Figure 1. IR spectra of the Co concentrate of 9:1 (NO_3:OAc) ratio (A), after heating at 3 °C min^{-1} to 95 °C (B), 265 °C (C), and 500 °C (D), and after heating at 10 °C min^{-1} to 120 °C (E) and 500 °C (F). (The phase evolution is discussed below.)

PXRD data characterizing these materials were very similar to those obtained from the TG batches (10−30 mg), and we may assume the materials to be very close to identical.

Cobalt films were prepared by spin-coating on alumina and alumium substrates at 2700 rpm for 30 s. After deposition, the concentrate films were heated in nitrogen to 500 °C at a rate of 10 °C min^{-1}. The films obtained after heat-treatment were investigated with SEM, TEM, and XRD.

Results and Discussion

Precursor Concentrate. After solvent evaporation, viscous purple-red concentrates remained. The viscosity of the concentrates differed somewhat, depending on the NO_3:OAc ratio, with the nitrate-rich concentrates being more fluid than those rich in acetate. The IR spectrum of the NO_3:OAc (9:1) ratio concentrate is shown in Figure 1. The peaks can be assigned as mainly due to: O−H stretching (3600−2800 cm^{-1}) and bending (1650−1550 cm^{-1}) in H_2O, N−O and C−O stretching in NO_3^- and OAc^-, (1550−1250 cm^{-1}), and C−C and C−O stretching (1053 and 1018 cm^{-1}) in TEA. The peaks assigned as due to C−C and C−O stretching in TEA were found at lower wavenumbers than in the free TEA (1074, 1035 cm^{-1}), which indicates that the TEA is bonded to the cobalt ions. Several small peaks in the region below 1250 cm^{-1} may be assigned to C−C and C−O bending in TEA, nitrate, and acetate groups and to different vibration modes of O−H groups, and to some extent Co−O stretching.[21] It seems reasonable to assume that very little or no decomposition occurred during solvent evaporation, leaving the TEA, acetato, and nitrato groups intact, although some loss of water, exchange of water for MeOH, and changes in ligand coordination modes might have taken place.

Sponge Preparation. Nitrate-to-Acetate Ratio. The TG studies at 10 °C min^{-1} showed that the nitrate:acetate ratio had a great influence on the decomposition process, as can be seen in Figure 2. The nitrate-rich compositions showed a rapid weight-loss step around 100 °C, followed by a plateau before the final weight-loss around 450 °C, whereas the most acetate-rich compositions had a stepwise decomposition, finishing at approximately the same temperature as that of the nitrate-rich mixtures. The samples heated at 10 °C min^{-1} to 700 °C in the pit-furnace had very low and seemingly random N and O contents, 0.02 and 0.2 wt %, respectively,

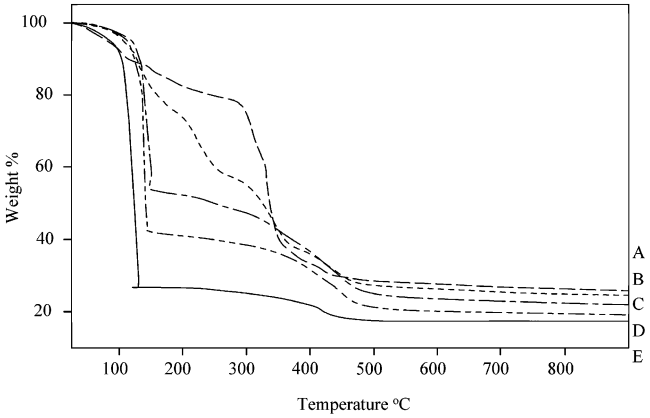

Figure 2. TG graphs of samples of different NO_3:OAc ratios, using a heating-rate of 10 °C min^{-1} in nitrogen atmosphere: 0:1 (A), 1:2 (B), 1:1 (C), 2:1 (D), and 1:0 (E).

Table 1. Elemental Analysis of Carbon Contents in Samples Prepared at 700 °C, versus NO_3:OAc Ratio in the Precursor Mixture

NO_3:OAc ratio	average wt % C	max. deviation from average (wt % units)	number of analyses
1:0	0.48	0.02	2
9:1	0.68		1
2:1	6.1	0.6	4
1:1	8.7	0.2	2
1:2	9.0	1.2	3
0:1	13.0		1

for the 1:0 sample. The carbon content increased with the acetate concentration from 0.5 wt % for the NO_3:OAc 1:0 composition to 13 wt % for the 0:1 composition as shown in Table 1.

The PXRD studies showed the exclusive presence of face centered cubic (fcc) cobalt for all NO_3 to OAc ratios.[22] Although the carbon content was lowest at the 1:0 composition, the 9:1 composition, yielding 0.7 wt % carbon, was chosen for more detailed studies of cobalt metal preparation, due its greater stability against crystallization, which occasionally occurred with solutions of the 1:0 composition.

Heating-Rate. The TG graphs of the 9:1 composition at different heating-rates showed two different decomposition patterns at the heating-rates 5 and 10 °C min^{-1}, as seen in Figure 3. During slow heating, the weight-loss progressed rather steadily up to 450 °C, whereas heating at 10 °C min^{-1} or more induced a rapid weight-loss at approximately 100

(21) Nakamoto, K. *Infrared and Raman Spectra of Inorganic and Coordination Compounds*, 4th ed.; Wiley−Interscience./John Wiley and Sons: Chichester, 1986.

(22) XRD JCPDS 15-806 Natl. Bur. Stand. (U. S.) Monogr. 25, 25 10, 1965.

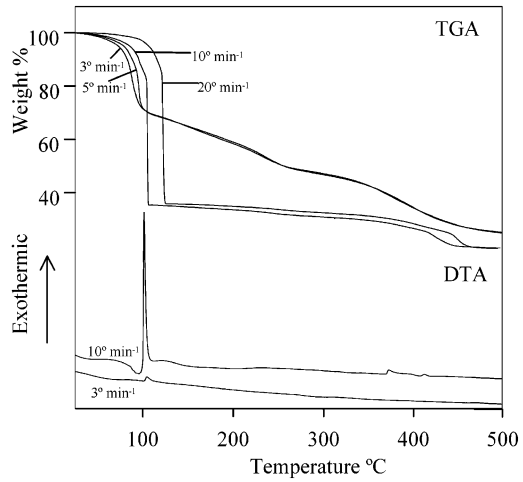

Figure 3. TG graphs obtained from an NO_3:OAc (9:1) sample, using the heating-rates 3, 5, 10, and 20 °C min^{-1}, and DTA graphs obtained using the heating-rates 3 and 10 °C min^{-1}, under nitrogen.

°C, followed by a plateau before a final small weight-loss occurred around 450 °C. The DTA curves also showed two different decomposition patterns, as can be seen in Figure 3. It can be noted that the low heating-rates produced a very small exothermic peak around 100 °C, followed by an almost constant heat-release up to 300 °C, whereas the higher heating-rates caused a very strong and sharp exothermic peak to occur at ca. 100 °C, followed by a broad exothermic peak at 100−250 °C and a few small exothermic peaks up to 450 °C. It is possible that, at the higher heating-rates, the mixture of oxidizing nitrate and reducing organic groups ignites and releases almost all of its energy in one step, and the plateau observed in the TG curve then indicates that the material is heated to ca. 350−400 °C. The high decomposition rate and heat-release in connection with substantial gas evolution probably inflates the viscous concentrate during the metal formation, and the escaping gases then immediately cause a rapid cooling, thereby freezing the observed nanophase sponge structure (vide infra). The following heating of the sponge to ca. 450 °C then slowly removes the residual groups or converts them to carbon, depending on the NO_3:OAc ratio. At lower heating-rates, the decomposition is more progressive and does not release enough heat to ignite the sample, resulting in a denser material.

Phase Evolution. Samples from different steps in the thermal decomposition were quenched and studied by IR spectroscopy (see Figure 1). With lower heating-rates, the amount of water and nitrate seems to be somewhat reduced after the first weight loss, up to 95 °C. The peaks associated with NO_3^- and OAc^- groups also changed slightly in shape, the maximum moved from 1382 to 1350 cm^{-1}, and the multiple peak at 1750−1500 cm^{-1} grew considerably in strength. This is probably due to a change in coordination mode of the nitrate and acetate groups, caused by the removal of coordinated water and leading to a more monodentate type of bonding of these groups.[21] After the second step, up to 265 °C, the peak in the 1750−1500 cm^{-1} region had grown even more in comparison with the other peaks, but absorptions associated with water, OAc^- and/or NO_3^- groups, and C−C and C−O stretching in TEA were still observed. The peak found at 2187 cm^{-1} is assigned to −CO and/or −NO groups coordinated to cobalt, stemming from decomposed nitrate and/or acetate groups. In the case of CO, the absorption maximum fits a linear coordination to a $CoO_{1-1.5}$ surface, according to the literature.[17] Further heating to 500 °C decomposed all nitrate and organic groups, and only extremely weak peaks presumably due to water absorbed on the metal when taken out of the TG-apparatus were observed.

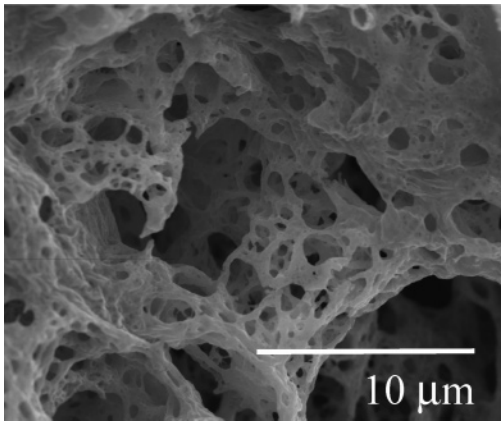

Figure 4. SEM image of cobalt sponge obtained after heating at 10 °C min^{-1} to 500 °C.

With the higher heating-rates, almost all groups were decomposed in one step at temperatures below 120 °C. The remaining weak peak at ca. 430 cm^{-1} is assigned to Co−O stretching in surface CoO, while the cobalt metal is impenetrable to the IR radiation. The remaining residual groups were removed after heating to 500 °C, and the peak ascribed to Co−O stretching was absent in this case. The very weak peaks observed in the sample heated to 120 °C at 10 °C min^{-1} were very similar to those found in the 265 °C sample heated at 3 °C min^{-1} and can be assigned in the same way.

Sponge Microstructure. The microstructure of the cobalt metal depended both on the heating-rate and on the final temperature. The SEM study of cobalt heated at 10 °C min^{-1} to 500 °C showed a very porous microstructure, with pore-sizes in a wide range on the micrometer scale as shown in Figure 4. The TEM studies of sponge powder that had been transferred from the TG apparatus to the TEM under inert atmosphere showed that the material consisted of ca. 50−100 nm thick walls of ca. 9−11 nm size and strongly coalesced cobalt crystallites as shown in Figure 5. The PXRD and electron diffraction patterns showed that the material consisted of fcc cobalt. The calculation of the grain-size using the Scherrer formula yielded the average grain-size of 10−12 nm, corroborating the TEM investigation. In some samples, however, a smaller and sharper peak superimposed on the broad peak corresponding to 9−11 nm of ca. 20 nm grain-size was observed. It is not known if the larger grain-size stems from the sample preparation including grinding and compaction, or if small amounts of 20 nm sized crystallites were present in the sample. Such crystallites should then be present in the junctions of the thin walls that are impenetrable to the electron-beam and thereby not possible to study with TEM.

The cobalt sponge is less stable toward oxidation in ambient atmosphere than the corresponding nickel sponge,[20]

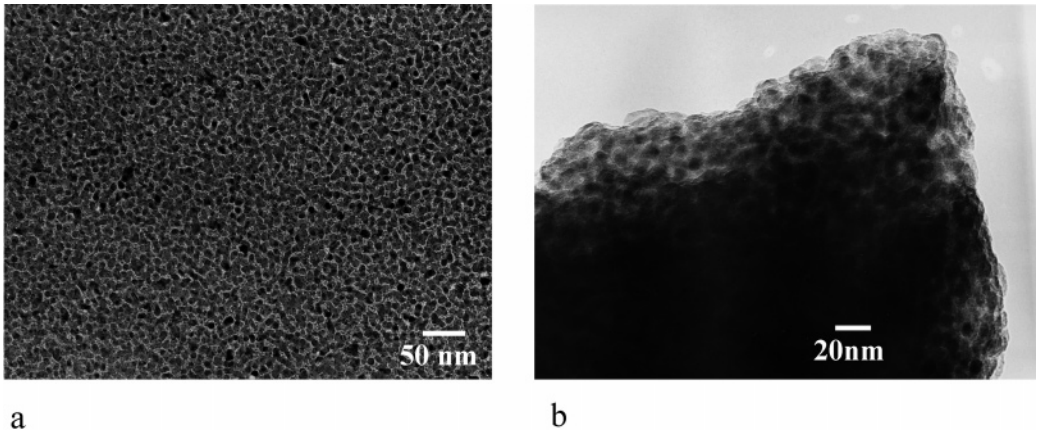

Figure 5. TEM images of cobalt sponge of 9−11 nm sized crystallites obtained after heating at 10 °C min^{-1} to 500 °C, showing a surface (A) and the ca. 60 nm thick side of the metal wall (B).

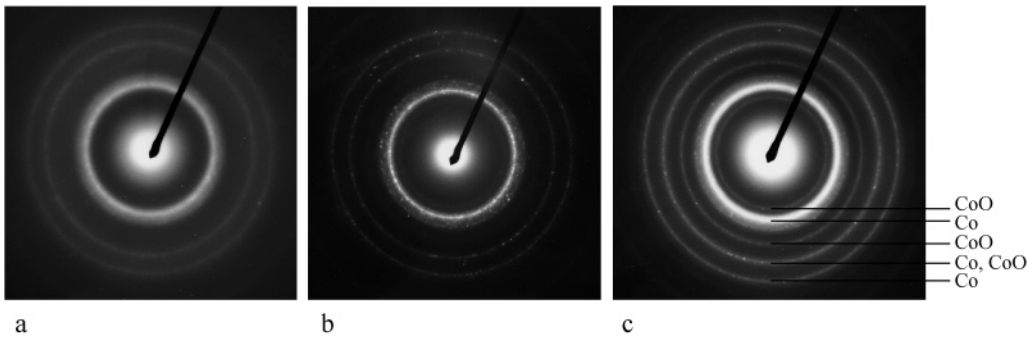

Figure 6. Electron-diffraction pattern of a sponge of 3−6 nm crystallites (A), sponge of 9−11 nm sized cobalt crystallites (B), and the same kind of sponge exposed to air (C).

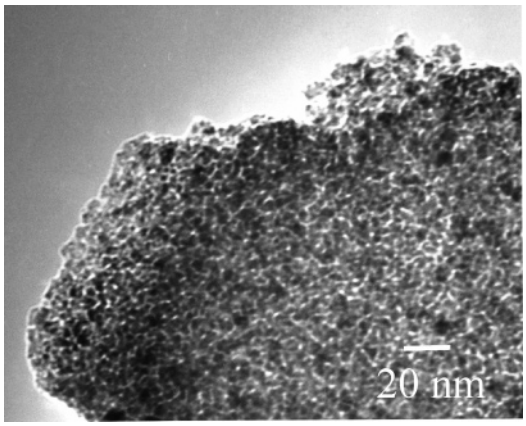

Figure 7. TEM images of cobalt sponge of 3−6 nm sized crystallites obtained after heating at 10 °C min^{-1} to 470 °C.

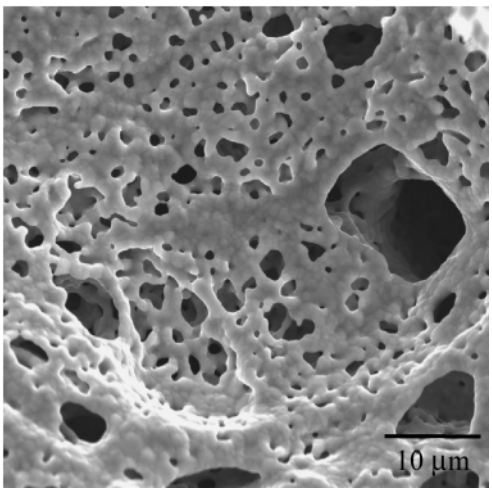

Figure 8. SEM image of cobalt sponge obtained after heating at 10 °C min^{-1} to 900 °C.

and the diffraction patterns showed rings from CoO in samples exposed to air for only a short time as shown in Figure 6c, although microstructural changes were not observed.

After being heated to temperatures in the range 400−470 °C, the selected area diffraction patterns showed rather diffuse ring structures as shown in Figure 6a, with the diffraction rings in the positions of fcc cobalt, indicating that the metal was amorphous or the crystallite sizes were ca. 1.5−2 nm or less. The observed material was composed of 3−6 nm sized and closely agglomerated particles as shown in Figure 7. This is similar to what was found for the nickel sponges heated to 400 °C.[20] A minor part of the material found in the thicker parts of the sponge consisted of ca. 10 nm sized cobalt crystals of the fcc modification.

The materials were still porous after heating to 900 °C, but, according to the SEM and TEM imaging, had sintered significantly to ca. 1−2 μm sized structures consisting of crystallites in the size range 5−200 nm, such as those seen in Figures 8 and 9.

Heating at 3 °C min^{-1} to 500 °C yielded a completely different microstructure, consisting of dense metal plates as shown in Figure 10. TEM studies showed that the crystal sizes were significantly larger and had a wider size distribution, 15−50 nm, than the sample prepared with a 10 °C

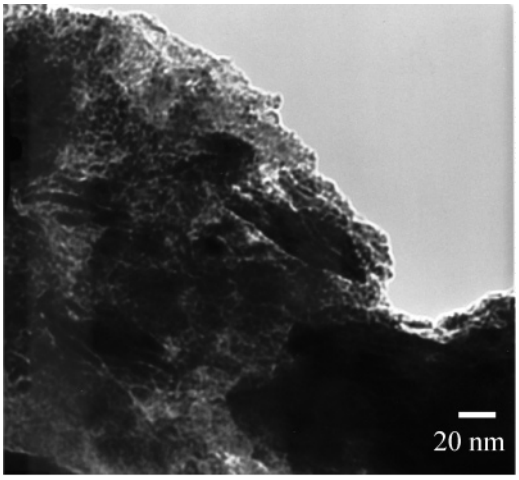

Figure 9. TEM image of cobalt sponge obtained after heating at 10 °C min^{-1} to 900 °C.

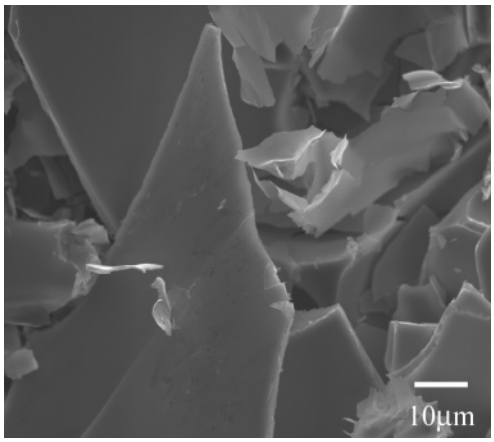

Figure 10. SEM image of cobalt obtained after heating at 3 °C min^{-1} to 500 °C.

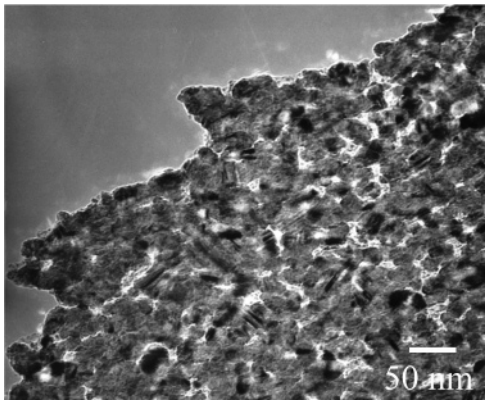

Figure 11. TEM image of cobalt obtained after heating at 3 °C min^{-1} to 500 °C.

min^{-1} heating-rate, as seen in Figure 11. In this case too, only fcc cobalt was obtained according to the PXRD and TEM-ED studies.

Film Preparation. The 150−200 nm thick films, obtained by spin-coating 1 M NO_3:OAc (9:1) solutions on polycrystalline α-alumina and alumium substrates and subsequent heating to 500 °C at 10 °C min^{-1}, were crack-free except in the ca. 1 mm wide outer rim of the film (Figure 12). The adherence to the substrates was excellent; the films were not removed by ripping off a well-attached scotch tape, and

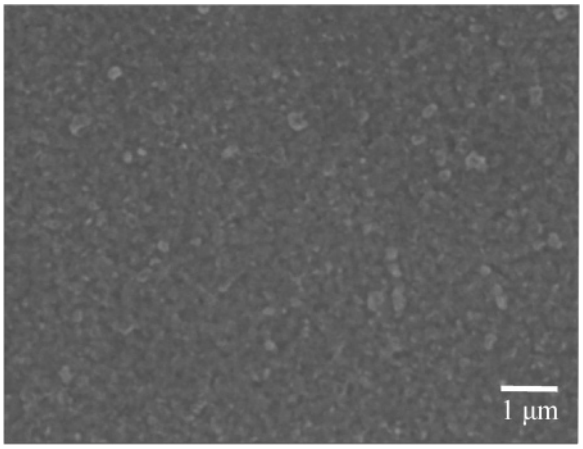

Figure 12. SEM image of cobalt film deposited on alumina, obtained after heating at 10 °C min^{-1} to 500 °C.

scratching with a scalpel was very difficult, normally leading to the substrate being removed together with the coating. It is interesting that a metal film can be deposited onto alumina, because metals are known to have a very low affinity to oxides and easily form droplets.[4,23] Possibly, kinetic factors play a role in that the metal is formed very rapidly from a viscous organic concentrate, and once the metal is formed as a film, the kinetic barrier against droplet formation is high. Preliminary tests showed that cobalt films could also be deposited on other substrates such as unpolished coarse-grained alumina, SnO_2:F coated glass, titanium and platinum. The TEM studies of pieces scratched off from the substrates showed that the films consisted of crystallites of sizes below 20 nm. The TEM-ED and XRD studies showed fcc cobalt as the only crystalline phase, and the amount of intergranular phase was small.

The formation of 150−200 nm thick, dense films from a solution under the conditions that yielded a porous sponge without the substrate may depend on the heated precursor liquid being well attached to the substrate during the formation of the metal, making bubble formation less probable and providing a more rapid cooling through the substrate. The metal film thickness is not much greater than the typical wall-thickness of the sponges prepared from thicker layers of precursor concentrate, and therefore formation of bubbles seem not to be necessary when the combustion gases are evolved from liquid precursor films.

The films were sensitive to oxidation, and CoO was found as a minority phase both in the TEM studies and in the XRD pattern after only a day in air. In films aged for months, the surface was completely oxidized, while the innermost part was still metallic. Attempts were made to increase the oxidation resistance by increasing the residual carbon content, using the more carbon-rich 3:1 NO_3:OAc ratio, but this film was also oxidized.

It is notable that although the hcp modification is stable below 420 °C and is normally obtained in large-grain bulk cobalt,[24,25] we obtained solely the fcc modification in all of our films and sponge samples. It appears from the literature

(23) Campbell, C. T. *Surf. Sci. Rep.* **1997**, *27*, 1−111.
(24) Ram, S. *Acta Mater.* **2001**, *49*, 2227−2307.
(25) Zhao, J.-C.; Notis, M. R. *Scr. Metall. Mater.* **1995**, *32*, 671−1676.

that with very thin films, below ca. 20−30 nm, and crystalline substrates that have a good attachment to the cobalt, the substrate structure is a strongly determining factor on the crystal phase obtained. With thicker films, the modification obtained depends on several factors such as deposition temperature and deposition technique, besides the crystallite size, and sometimes mixtures of phases are obtained.[4−8,10,15] It also seems probable that factors such as the amount of intergranular amorphous cobalt phase, intermixing with the metallic substrates, and surface contamination by, for example, C, CO, O, and borate or sulfate groups in electrodeposition may play a role in the crystallization and stabilization of different cobalt modifications. In our method, it is possible that the first cobalt clusters formed are covered with different groups such as acetate, nitrate, CO, NO, and partly decomposed TEA, which later evaporate or are converted to carbon in amounts depending on the OAc:NO_3 ratio. It has been shown that on alumina substrates, which have a very low affinity to cobalt, and with cobalt of very small particle sizes, the fcc modification is consistently obtained.[4] This case is probably close to our sponges and films where the crystals probably nucleate homogeneously within a liquid, without any substrate influence.

Conclusion

Nanophase fcc cobalt in the forms of highly porous sponges and films has been obtained via a new solution-chemical route, after heating to 500 °C in nitrogen. Different morphologies can be obtained by using different heating-rates. Thus, sponges of 9−11 nm sized fcc cobalt crystallites were formed in samples heated to 500 °C at 10 °C min^{-1}, whereas heating to the same temperature at 3 °C min^{-1} yielded dense plates of 15−50 nm sized crystallites. At lower temperatures, amorphous and 3−6 nm sized crystalline particles can be obtained. Using different nitrate-to-acetate ratios in the precursor mixtures could serve to control the carbon content in the sponges. Films of 150−200 nm thickness, consisting of <20 nm sized crystallites, were obtained by spin-coating and heating to 500 °C on a number of substrates known to be difficult for metal deposition.

This very efficient route, using only cheap inorganic and organic compounds, should be very suitable for large-scale production of both films and high-surface-area electrodes and catalysts. The nanophase sponge might also be used as a starting material for nanostructured cobalt compacts, which is a possibility that we are presently investigating.

Acknowledgment. We thank The Swedish Science Council (VR) for financing this study. The researchers involved in this work are affiliated with the VINNOVA Brinell Centre, Inorganic Interfacial Engineering.

CM0494610